C–C and C–N Couplings Following Hydride Addition on Isocyanide Cyclopolyenyl Dimolybdenum Complexes to Give Tethered Aldimine and Aminocarbene Derivatives

Belén Alvarez, M. Angeles Alvarez, M. Esther García, Daniel García-Vivó,* and Miguel A. Ruiz*[a]

Abstract: Reaction of $[Mo_2Cp_2(\mu\text{-}\kappa^1\text{:}\kappa^1,\eta^6\text{-PMes*})(CO)_2]$ with S or Se followed by protonation with $[H(OEt_2)_2](BAr'_4)$ gave the cationic derivatives $[Mo_2Cp_2\{\mu\text{-}\kappa^2_{P,E}\text{:}\kappa^1_P,\eta^5\text{-EP}(C_6H_3t\text{Bu}_3)\}(CNR)(CO)_2](BAr'_4)$ (E = S; R = *t*Bu, *i*Pr, Ph, 4-C_6H_4OMe, Xyl. E = Se; R = *t*Bu. Ar′ = 3,5-$C_6H_3(CF_3)_2$). Reaction of the latter with $K[BHsBu_3]$ yielded the aldimine complexes $[Mo_2Cp_2\{\mu\text{-}\kappa^2_{P,E}\text{:}\kappa^2_{P,N},\eta^4\text{-SP}(C_6H_3t\text{Bu}_3(CHNR))\}(CO)_2]$ and their aminocarbene isomers $[Mo_2Cp_2\{\mu\text{-}\kappa^2_{P,E}\text{:}\kappa^2_{P,C},\eta^4\text{-SP}(C_6H_3t\text{Bu}_3(NRCH))\}(CO)_2]$ (R ≠ Xyl), following respectively from C–C and C–N couplings. Monitoring of these reactions revealed that the initial H^- attack takes place at a Cp ligand, to give cyclopentadiene intermediates $[Mo_2Cp\{\mu\text{-}\kappa^2_{P,S}\text{:}\kappa^1_P,\eta^5\text{-SP}(C_6H_3{}^t\text{Bu}_3)\}(\eta^4\text{-}C_5H_6)(CNR)(CO)_2]$ which then undergo C–H oxidative addition to give the hydride isomers $[Mo_2Cp_2\{\mu\text{-}\kappa^2_{P,S}\text{:}\kappa^1_P,\eta^3\text{-SP}(C_6H_3{}^t\text{Bu}_3)\}(H)(CNR)(CO)_2]$. The latter in turn rearrange to give the aldimine and aminocarbene complexes. DFT calculations revealed that the hydride intermediates first undergo migratory insertion of the isocyanide ligand into the Mo–H bond, to give unobservable formimidoyl intermediates which then evolve either by the nucleophilic attack of the N atom to the C_6 ring (C–N coupling), or by the migratory insertion of the formimidoyl ligand to the C_6 ring (C–C coupling). Our data suggest that increasing the size of the substituent R at the isocyanide ligand de-stabilizes the aldimine isomer to a greater extent, then favoring the formation of the aminocarbene complex.

Introduction

The reactions of coordinated hydrocarbon groups on the coordination sphere of transition-metal atoms are at the very heart of organometallic chemistry,[1] and constitute useful synthetic strategies to prepare new organic molecules and also novel polyfunctional ligands which can modulate the chemical behavior of metal complexes in many different ways, particularly in catalytic processes.[2,3] Classic examples of this sort of reactions are the nucleophilic and electrophilic attacks of different reagents on polyene and polyenyl metal complexes.[1] Recently, while studying the reactivity of dimolybdenum complexes bridged by arylthiophosphinidene ligands we discovered that the stepwise addition of H^+ and H^- on complex *syn*-$[Mo_2Cp_2(\mu\text{-}\kappa^2_{P,S}\text{:}\kappa^1_P,\eta^4\text{-SPMes*})(CN\text{t}Bu)(CO)_2]$ accomplished rare hydroamination and hydrocarbation processes on the uncoordinated C=C double bond of the aryl ligand at the parent substrate, to yield complexes bearing aldimine and aminocarbene groups tethered to a η^4-cyclohexadiene ring.[4]

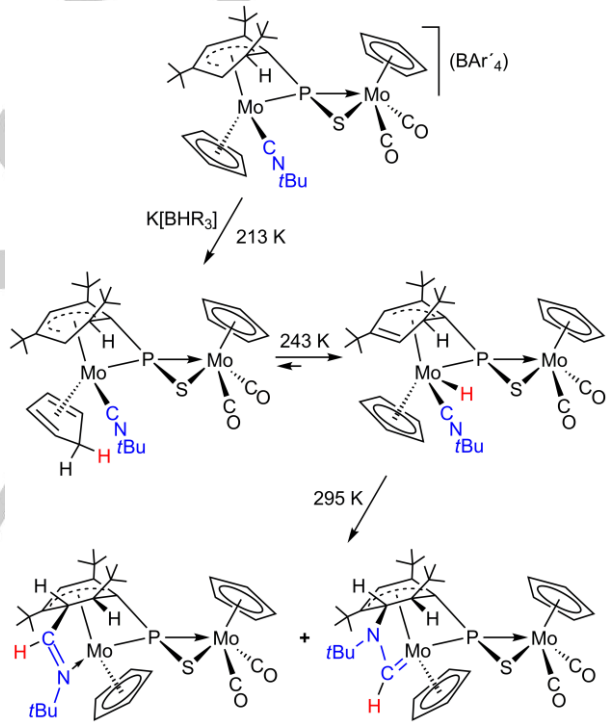

Scheme 1. Preliminary studies on the CN*t*Bu complex (R = *s*Bu)

Very unexpectedly, a spectroscopic monitoring on the second step of this reaction revealed the intermediacy of cyclopentadiene and hydride intermediates following hydride attack on the cation that arouse from the first (protonation) step (Scheme 1). There were several aspects of interest in these transformations: In the first place, the fact that hydride attack was initiated at the cyclopentadienyl ligand was surprising, since the C^5 atom of the C_6 ring of the thiophosphinidene ligand would have been predicted as the preferred site for nucleophilic attack on the basis of the Davies-Green-Mingos rules.[5] Secondly, even if the C to M hydrogen transfer involved in the transformation of the observed cyclopentadiene intermediate into the corresponding cyclopentadienyl hydride isomer is a process previously proposed to take place in different

[a] Dr. B. Alvarez, Dr. M. A. Alvarez, Prof. Dr. M. E. García, Dr. D. García-Vivó, Prof. Dr. M. A. Ruiz
Departamento de Química Orgánica e Inorgánica/IUQOEM
Universidad de Oviedo
E-33071 Oviedo, Spain
E-mail: garciavdaniel@uniovi.es (D.G.V.), mara@uniovi.es (M.A.R.)

Supporting information for this article is given via a link at the end of the document.

nucleophilic addition and functionalization reactions of cyclopentadienyl complexes,[6,7] an equilibrium between this sort of isomers seems to have been never observed before. Thirdly, the formation of the imine product required the insertion of a formimidoyl group into a M–C(sp^2) bond of a polyenyl ligand, a C–C coupling event previously reported only for metal–alkyl bonds.[8] And finally, as concerning the C–N coupling leading to the aminocarbene ligand tethered to the cyclohexadiene ring we note that, to our knowledge, the nucleophilic attack of the N atom of a formimidoyl or iminoacyl ligand to a metal-bound polyene group has been neither reported previously. Based on all the above considerations, we then decided to get more insight into these intricate transformations by extending our studies to related cationic Mo_2 complexes bearing isocyanide ligands other than CN*t*Bu, and by analyzing, using Density Functional Theory (DFT) methods, the elemental steps connecting the initial cyclopentadiene intermediates to the aldimine and aminocarbene complexes eventually isolated, both from thermodynamic and kinetic points of view. This would allow us to check the influence of the isocyanide ligand on these unusual reactions and might also provide us with valuable information to rationalize their outcome, and perhaps also to grasp the key factors governing the critical C–C and C–N coupling steps dictating the nature of the final products. As it will be shown below, the above transformations proved to be quite general and most influenced by the size of the substituent at the isocyanide ligand, which generally favored the formation of the aminocarbene complexes, while the flexible hapticity of the C_6 ring of the thiophosphinidene ligand had a relevant role in facilitating the long hydrogen trip from the Cp up to the isocyanide ligand, as required to yield the final products.

Results and Discussion

Preparation and structural characterization of cationic isocyanide precursors

The cationic isocyanide complex $[Mo_2Cp_2\{\mu\text{-}\kappa^2_{P,S}\text{:}\kappa^1_P,\eta^5\text{-}SP(C_6H_3tBu_3)\}(CNtBu)(CO)_2](BAr'_4)$ (**2a**) used in our preliminary report[4] was prepared through protonation of the corresponding neutral thiophosphinidene complex *syn*-$[Mo_2Cp_2(\mu\text{-}\kappa^2_{P,S}\text{:}\kappa^1_P,\eta^4\text{-}SPMes^*)(CNtBu)(CO)_2]$ (**1a**), a molecule in turn made through the reaction of the phosphinidene complex $[Mo_2Cp_2(\mu\text{-}\kappa^1\text{:}\kappa^1,\eta^6\text{-}PMes^*)(CO)_2]$ with elemental sulfur in the presence of CN*t*Bu.[9] We have now used a similar procedure to prepare related complexes with different substituents at the isocyanide ligand (Scheme 2). Indeed, the reaction of the mentioned phosphinidene complex with elemental sulfur in the presence of CNR yielded the corresponding thiophosphinidene derivatives *syn*-$[Mo_2Cp_2(\mu\text{-}\kappa^2_{P,S}\text{:}\kappa^1_P,\eta^4\text{-}SPMes^*)(CNR)(CO)_2]$ (R = *i*Pr (**1b**), Ph (**1c**), 4-C_6H_4OMe (**1d**), Xyl (**1e**)) in a regioselective way (Xyl = 2,6-$C_6H_3Me_2$). Subsequent protonation of the latter complexes with $[H(OEt_2)_2](BAr'_4)$ yielded the corresponding cyclohexadienyl derivatives $[Mo_2Cp_2\{\mu\text{-}\kappa^2_{P,S}\text{:}\kappa^1_P,\eta^5\text{-}SP(C_6H_3tBu_3)\}(CNR)(CO)_2](BAr'_4)$ (**2b-e**) almost quantitatively (Ar´= 3,5-$C_6H_3(CF_3)_2$). This procedure could also be extended to the related selenophosphinidene complex *syn*-$[Mo_2Cp_2(\mu\text{-}\kappa^2_{P,Se}\text{:}\kappa^1_P,\eta^4\text{-}SePMes^*)(CNtBu)(CO)_2]$, which was protonated analogously to yield the corresponding hexadienyl derivative $[Mo_2Cp_2\{\mu\text{-}\kappa^2_{P,Se}\text{:}\kappa^1_P,\eta^5\text{-}SeP(C_6H_3tBu_3)\}(CNtBu)(CO)_2](BAr'_4)$ (**3**) in good yield. We recall here that a detailed experimental and theoretical study of the protonation reactions of the CN*t*Bu complex **1a** revealed that this reaction is initiated by proton attack at the sulfur atom, this being followed then by a H-shift to the arene ligand, thus justifying its *endo* position in the final cyclohexadienyl complex.[10]

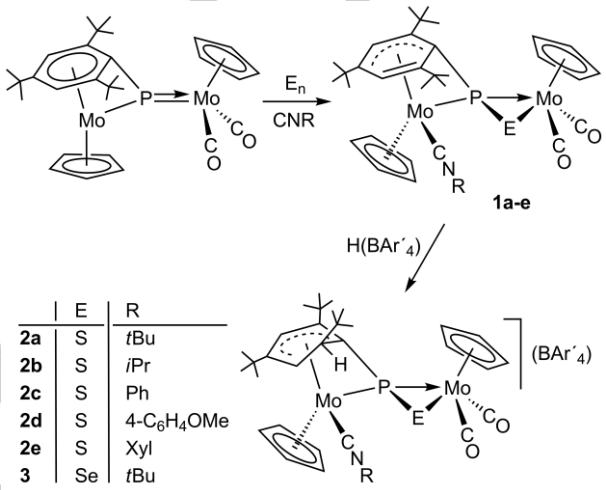

	E	R
2a	S	*t*Bu
2b	S	*i*Pr
2c	S	Ph
2d	S	4-C_6H_4OMe
2e	S	Xyl
3	Se	*t*Bu

Scheme 2

Spectroscopic data for compounds **1b-e** (Table 1 and Experimental Section) are comparable to those of the CN*t*Bu complex **1a** and deserve no detailed comments. We note that an X-ray diffraction study on the latter species, which is identified by a ^{31}P NMR resonance at 73.8 ppm, confirmed a proximal (*syn*) disposition of the CN*t*Bu ligand with respect to the sulfur atom, while the alternative isomer displaying an *anti* arrangement of the CN*t*Bu ligand (relative to S) displayed a resonance at 98.4 ppm.[9] Thus, the ^{31}P chemical shifts of ca. 75 ppm for all compounds **1b-e** ensure that *syn* isomers have been formed in all cases. Another possible isomerism in this sort of molecules arises from the relative arrangement (*cis* or *trans*) of the Cp rings relative to the MoPS plane, but the spectroscopic data for **1a** proved that only the *trans* isomer is present in solution for **1a**,[9] and the same is assumed to be the case for compounds **1b-e**.

Table 1. Selected IR[a] and $^{31}P\{^{1}H\}$ NMR Data[b] for New Compounds.

Compound	ν(CN)	ν(CO)	δ(P)
syn-[$Mo_2Cp_2(\mu\text{-}\kappa^2_{P,S}{:}\kappa^1_P,\eta^4$-SPMes*)(CN*t*Bu)$(CO)_2$] (**1a**)[c]	2134 (m)	1921 (vs), 1833 (s)	73.8[d]
syn-[$Mo_2Cp_2(\mu\text{-}\kappa^2_{P,S}{:}\kappa^1_P,\eta^4$-SPMes*)(CN*i*Pr)$(CO)_2$] (**1b**)	2142 (m)	1923 (vs), 1835 (s)	74.9
syn-[$Mo_2Cp_2(\mu\text{-}\kappa^2_{P,S}{:}\kappa^1_P,\eta^4$-SPMes*)(CNPh)$(CO)_2$] (**1c**)	2096 (m)	1926 (vs), 1838 (s)	75.0
syn-[$Mo_2Cp_2(\mu\text{-}\kappa^2_{P,S}{:}\kappa^1_P,\eta^4$-SPMes*){CN(4-$C_6H_4$OMe)}$(CO)_2$] (**1d**)	2103 (s)	1925 (vs), 1838 (s)	75.0
syn-[$Mo_2Cp_2(\mu\text{-}\kappa^2_{P,S}{:}\kappa^1_P,\eta^4$-SPMes*)(CNXyl)$(CO)_2$] (**1e**)	2074 (s)	1925 (vs), 1838 (s)	75.5
[$Mo_2Cp_2\{\mu\text{-}\kappa^2_{P,S}{:}\kappa^1_P,\eta^5$-SP($C_6H_3t Bu_3$)}(CN*t*Bu)$(CO)_2$](BAr´$_4$) (**2a**)[e]	2177 (m)	1955 (vs), 1877 (s)	108.1
[$Mo_2Cp_2\{\mu\text{-}\kappa^2_{P,S}{:}\kappa^1_P,\eta^5$-SP($C_6H_3t Bu_3$)}(CN*i*Pr)$(CO)_2$](BAr´$_4$) (**2b**)	2182 (m)	1955 (vs), 1875 (s)	108.4
[$Mo_2Cp_2\{\mu\text{-}\kappa^2_{P,S}{:}\kappa^1_P,\eta^5$-SP($C_6H_3t Bu_3$)}(CNPh)$(CO)_2$](BAr´$_4$) (**2c**)	2151 (m)	1956 (vs), 1877 (s)	109.2
[$Mo_2Cp_2\{\mu\text{-}\kappa^2_{P,S}{:}\kappa^1_P,\eta^5$-SP($C_6H_3t Bu_3$)}{CN(4-$C_6H_4$OMe)}$(CO)_2$](BAr´$_4$) (**2d**)	2151 (w)	1955 (vs), 1877 (s)	109.3
[$Mo_2Cp_2\{\mu\text{-}\kappa^2_{P,S}{:}\kappa^1_P,\eta^5$-SP($C_6H_3t Bu_3$)}(CNXyl)$(CO)_2$](BAr´$_4$) (**2e**)	2144 (m)	1956 (vs), 1878 (s)	111.1
[$Mo_2Cp_2\{\mu\text{-}\kappa^2_{P,Se}{:}\kappa^1_P,\eta^5$-SeP($C_6H_3t Bu_3$)}(CN*t*Bu)$(CO)_2$](BAr´$_4$) (**3**)	2176 (m)	1954 (vs), 1877 (s)	125.0[f]
[$Mo_2Cp_2\{\mu\text{-}\kappa^2_{P,S}{:}\kappa^2_{P,N},\eta^4$-SP($C_6H_3t Bu_3$(CHN*t*Bu))}$(CO)_2$] (**6a**)[g]		1921 (vs), 1834 (s)	115.0
[$Mo_2Cp_2\{\mu\text{-}\kappa^2_{P,S}{:}\kappa^2_{P,N},\eta^4$-SP($C_6H_3t Bu_3$(CHN*i*Pr))}$(CO)_2$] (**6b**)		1921 (vs), 1833 (s)	113.2
[$Mo_2Cp_2\{\mu\text{-}\kappa^2_{P,S}{:}\kappa^2_{P,N},\eta^4$-SP($C_6H_3t Bu_3$(CHNPh))}$(CO)_2$] (**6c**)		1923 (vs), 1837 (s)	118.6
[$Mo_2Cp_2\{\mu\text{-}\kappa^2_{P,S}{:}\kappa^2_{P,N},\eta^4$-SP($C_6H_3t Bu_3$(CHN(4-$C_6H_4$OMe)))}$(CO)_2$] (**6d**)		1923 (vs), 1837 (s)	118.5
[$Mo_2Cp_2\{\mu\text{-}\kappa^2_{P,S}{:}\kappa^2_{P,N},\eta^4$-SP($C_6H_3t Bu_3$(CHNXyl))}$(CO)_2$] (**6e**)		1926 (vs), 1839 (s)	105.7
[$Mo_2Cp_2\{\mu\text{-}\kappa^2_{P,S}{:}\kappa^2_{P,N},\eta^4$-SP($C_6H_3t Bu_3$(CHN*n*Bu))}$(CO)_2$] (**6f**)		1922 (vs), 1834 (s)	117.0
[$Mo_2Cp_2\{\mu\text{-}\kappa^2_{P,S}{:}\kappa^2_{P,C},\eta^4$-SP($C_6H_3t Bu_3$(N*t*BuCH))}$(CO)_2$] (**7a**)[g]		1921 (vs), 1834 (s)	118.5
[$Mo_2Cp_2\{\mu\text{-}\kappa^2_{P,S}{:}\kappa^2_{P,C},\eta^4$-SP($C_6H_3t Bu_3$(N*i*PrCH))}$(CO)_2$] (**7b**)		1922 (vs), 1834 (s)	121.9
[$Mo_2Cp_2\{\mu\text{-}\kappa^2_{P,S}{:}\kappa^2_{P,C},\eta^4$-SP($C_6H_3t Bu_3$(NPhCH))}$(CO)_2$] (**7c**)		1925 (vs), 1838 (s)	120.1
[$Mo_2Cp_2\{\mu\text{-}\kappa^2_{P,S}{:}\kappa^2_{P,C},\eta^4$-SP($C_6H_3t Bu_3$(N(4-$C_6H_4$OMe)CH))}$(CO)_2$] (**7d**)		1925 (vs), 1837 (s)	121.1
[$Mo_2Cp_2\{\mu\text{-}\kappa^2_{P,Se}{:}\kappa^2_{P,N},\eta^4$-SeP($C_6H_3t Bu_3$(CHN*t*Bu))}$(CO)_2$] (**8**)		1921 (vs), 1836 (s)	139.2[h]
[$Mo_2Cp_2\{\mu\text{-}\kappa^2_{P,Se}{:}\kappa^2_{P,C},\eta^4$-SeP($C_6H_3t Bu_3$(N*t*BuCH))}$(CO)_2$] (**9**)		1921 (vs), 1835 (s)	141.0[i]
[$Mo_2Cp_2\{\mu\text{-}\kappa^2_{P,S}{:}\kappa^2_{P,O},\eta^4$-SP($C_6H_3t Bu_3$(CHO))}$(CO)_2$] (**10**)		1928 (vs), 1842 (s)[j]	117.8

[a] Recorded in dichloromethane solution, with C–O stretching bands [ν(CO)] in cm^{-1}. [b] Recorded in CD_2Cl_2 solution at 121.51 MHz and 293 K unless otherwise stated. [c] Data taken from reference 9. [d] In C_6D_6 solution. [e] Data taken from reference 10. [f] $^1J(P, ^{77}Se)$ = 450 Hz. [g] Data taken from reference 4. [h] $^1J(P, ^{77}Se)$ = 412 Hz. [i] $^1J(P, ^{77}Se)$ = 421 Hz. [j] ν(C=O) = 1601 cm^{-1} (w)

Spectroscopic data for compounds **2b-e** and **3** (Table 1 and Experimental Section) also are comparable to those of the corresponding CN*t*Bu complex **2a**,[10] and consistent with the X-ray structure determined for the latter species in our preliminary report,[4] therefore only a few comments are to be made. Protonation of the neutral parent substrates induces considerable spectroscopic changes. Thus, in addition to a significant deshielding of some 35 ppm in the corresponding ^{31}P NMR resonance, we note a significant increase in the average C–O stretches of the carbonyl ligands (by ca. 35 cm^{-1}), which becomes even larger (45-70 cm^{-1}) for the C–N stretch of the isocyanide ligand bound to the metallocene fragment (usually a parameter less sensitive to charge changes). This is suggestive of the occurrence of a larger depletion of charge at this fragment (relative to the metal carbonyl fragment) as a result of protonation. The added proton atom in compounds **2b-e** gives rise to a new sp^3-hybridized CHR group, identified by the presence of relatively shielded CH resonances at ca. 3.7 ppm (^1H) and 58 ppm (^{13}C) in the corresponding NMR spectra, with the proton displaying a coupling of 6 Hz to the vicinal H of the ring, as usually observed for *endo* H atoms in η^4-bound hexadiene complexes.[11] Spectroscopic data for the selenophosphinidene complex **3** are comparable to those of the thiophosphinidene analogues **2** and deserve no particular comment. We just note that it displays a somewhat more deshielded ^{31}P NMR resonance (δ_P 125.0 ppm) exhibiting a large one-bond coupling of 450 Hz to the ^{77}Se nucleus, similar to the one observed for its neutral precursor (430 Hz).[9]

Hydride addition to compounds 2 and 3

As noted above, in our preliminary investigation we found that the reaction of K[$BHsBu_3$] with the cationic CN*t*Bu complex **2a** in THF solution proceeded *via* cyclopentadiene and hydride intermediates (compounds **4a** and **5a**, to be discussed later on) to eventually render a mixture of two products: the aldimine complex [$Mo_2Cp_2\{\mu\text{-}\kappa^2_{P,S}{:}\kappa^2_{P,N},\eta^4$-SP($C_6H_3t Bu_3$(CHN*t*Bu))}$(CO)_2$]

(**6a**), and its aminocarbene isomer [$Mo_2Cp_2\{\mu\text{-}\kappa^2_{P,S}\text{:}\kappa^2_{P,C},\eta^4\text{-}SP(C_6H_3tBu_3(NtBuCH))\}(CO)_2$] (**7a**), both of which were fully characterized both in solution and in the solid state at the time.[4] We have now examined the reactions of K[BHsBu_3] with the isocyanide complexes **2b-e**, and found that they proceed analogously to give mixtures of the corresponding aldimine (**6**) and aminocarbene (**7**) derivatives, in relative amounts depending on the particular isocyanide ligand, with a limiting case found for the CNXyl complex, which rendered no aminocarbene derivative (Figure 1). A similar behavior was found for the selenophosphinidene complex **3**, which reacted with K[BHsBu_3] to give also a mixture of the corresponding aldimine (**8**) and aminocarbene (**9**) derivatives (**8**/**9** ratio = 1/2). Thus, it seems that the nature of the chalcogen in these substrates only has a modest influence on the product distribution, while the substituent at the isocyanide ligand has a considerable, even determinant influence on it, with the bulkier *t*Bu and Xyl groups seemingly disfavoring (even precluding) the formation of the aminocarbene complexes, while electron-releasing substituents seem to favor them. Finally, we have also examined the reactions of compound **2a** with hydride sources different from K[BHsBu_3], and found that its reaction with Li[BHEt_3] yielded a **6a**/**7a** mixture essentially identical to the one formed when using K[BHsBu_3]. In contrast, the reaction with solid KH in THF solution gave a complex mixture of products that could not be identified. Therefore, it can be additionally guessed that steric factors also play a relevant role as concerning the selectivity of the initial hydride attack on the cationic complexes of type **2**.

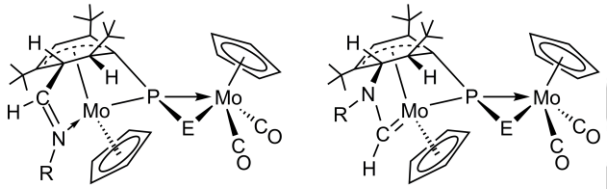

6a-e(S), **8**(Se) **7a-d**(S), **9**(Se)

	E	R	**6** / **7**
a	S	*t*Bu	1 / 2.5
b	S	*i*Pr	1 / 4
c	S	Ph	1.3 / 1
d	S	4-C_6H_4OMe	2.2 / 1
e	S	Xyl	1 / 0

Figure 1. Structures of compounds **6** to **9**.

Aldimine/Aldehyde transformations at the tethered group of compounds 6

Most compounds **6** and **7** mentioned above are not particularly air- or water-sensitive products. An exception to this behavior, however, was found for the aldimine complex **6e** having the very bulky Xyl group, which underwent progressive hydrolysis upon manipulation, to give the aldehyde complex [$Mo_2Cp_2\{\mu\text{-}\kappa^2_{P,S}\text{:}\kappa^2_{P,O},\eta^4\text{-}SP(C_6H_3tBu_3(CHO))\}(CO)_2$] (**10**) (Scheme 3), a reaction which could be carried out on a preparative scale by reacting **6e** with water in the presence of benzoic acid acting as a catalyst. We note that, in spite of the general fact that organic carbonyl functions are rather poor *O*-donor groups for low-valent organomolybdenum complexes, this does not seem to be the case in compound **10**, since this complex did not react with CO (3 atm) at room temperature upon prolonged exposure times. On the other hand, we should remark that compound **10** cannot be obtained through the preparative route leading to compounds **6**: actually, the reaction of [$Mo_2Cp_2\{\mu\text{-}\kappa^2_{P,S}\text{:}\kappa^1_{P},\eta^5\text{-}SP(C_6H_3tBu_3)\}(CO)_3$]($BAr'_4$) (the carbonyl analogue of complexes **2**)[10] with K[BHsBu_3] under similar conditions only yielded a mixture of unstable species which could not be properly isolated nor structurally characterized.

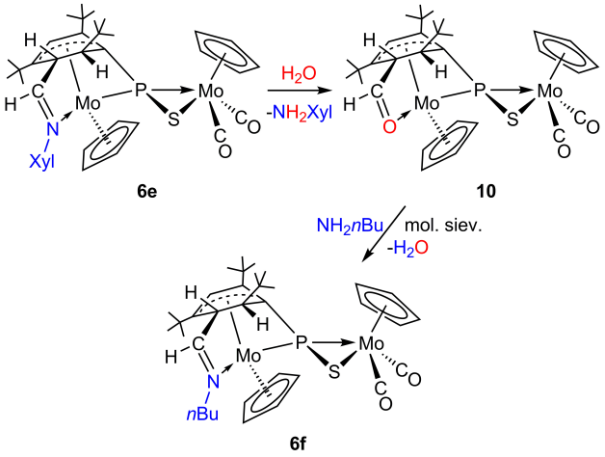

Scheme 3. Aldimine/aldehyde transformations of compounds **6**

Interestingly, the aldimine/aldehyde transformation leading to complex **10** could be reversed upon reaction of the latter compound with primary amines. Thus, the room temperature reaction of **10** with excess NH_2nBu (10 equiv) slowly yielded the corresponding aldimine complex [$Mo_2Cp_2\{\mu\text{-}\kappa^2_{P,S}\text{:}\kappa^2_{P,N},\eta^4\text{-}SP(C_6H_3tBu_3(CHNnBu))\}(CO)_2$] (**6f**), a product displaying spectroscopic properties analogous to compounds **2a-e**, therefore isostructural to them. The formation of **6f** requires the elimination of water, and indeed was best completed in the presence of 4 Å molecular sieves acting as a dehydration reagent (Scheme 3). We finally note that the above transformations are reminiscent of those of free aldehydes and ketones, which are known to react reversibly with primary amines to give the corresponding imine derivatives and water.[12] Such imine/carbonyl relationship is also known to be operative for transition-metal coordinated imine-donor ligands.[13]

Structural characterization of compounds 6, 8 and 10

The molecular structure of the aldimine complex **6a** was briefly described in our preliminary report on these reactions,[4] and we have now determined the structure of the related aldehyde complex **10**, which displays similar geometrical features (Figure 2 and Table 2).

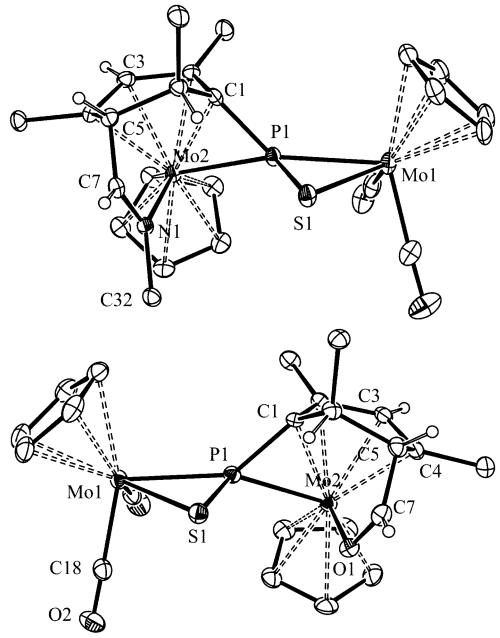

Figure 2. ORTEP diagrams (30% probability) of compounds **6a** (upper) and **10** (lower), with most H atoms and *t*Bu groups (except their C^1 atoms) omitted for clarity

Both molecules are built from MoCp and $MoCp(CO)_2$ fragments bridged by a thiophosphinidene ligand *P*,*S*-bound to the Mo atom bearing the terminal carbonyls, then completing a classical four-legged piano stool geometry around that metal center, which implies that the P atom is placed *cis* to one carbonyl ligand (P–Mo–C ca. 77°) and *trans* to the other one (P–Mo–C ca. 105°). The thiophosphinidene ligand is connected to the second metal atom *via* the P atom and its cyclohexadienyl substituent, the latter bound in a η^4-fashion, with Mo2–C lengths in the range 2.22-2.35 Å. The coordination sphere at the second Mo atom is completed by the κ^1-binding of the aldimine (**6a**) or aldehyde (**10**) groups tethered to the C^5 atom of the former aryl ring of the phosphorus ligand, which define similar angles of ca. 84° with the P atom. Dimensions within the PSMo ring in complexes **6a** and **10** are comparable to those previously measured in parent phosphinidene complexes of type **1**,[9] and deserve no particular comments. For compound **6a**, the C7 and N1 atoms of the aldimine ligand display trigonal environments as expected, and the C–N length of 1.277(4) Å compares well with the reference value of ca. 1.26 Å for a double bond between these atoms,[14] or the corresponding values measured in previous molybdenum cyclopentadienyl complexes bearing κ^1-aldimine ligands (cf. 1.270(16) Å in $[MoCp(CO)_2\{\kappa^2\text{-}NC_5H_4CH{=}N(CHMePh)\}]PF_6$),[15] but the Mo–N length of 2.287(3) Å is somewhat longer than expected (cf. 2.182(10) Å in the mentioned complex). This suggests a weakened aldimine coordination, likely due to the presence of the bulky *t*Bu group attached to the N atom, in line with DFT calculations to be discussed later on. Such a weakening effect expectedly would be even larger in the xylyl-bearing complex **6e**, perhaps justifying its higher susceptibility to hydrolysis. In contrast, these steric effects are obviously absent for the aldehyde complex **10**, with an *O*-bound atom devoid of any further substituent. In agreement with it, the Mo2–O length of 2.159(3) Å is comparable to the corresponding lengths in related κ^1-aldehyde or ketone complexes (cf. 2.179(5) Å in $[WCp(CO)_3(\kappa^1\text{-}OCHPh)](CF_3SO_3)$,[16] and an average of ca. 2.16 Å in $[Mo(\eta^5\text{-}C_5Bz_5)(CO)_3(\kappa^1\text{-}OCMe_2)]BF_4$),[17] while the C–O length of 1.235(5) Å compares well with the double-bond reference value of ca. 1.21 Å.[14]

Table 2. Selected Bond Lengths (Å) and Angles (°) for Compounds **6a** and **10**

	6a[4]	**10**
Mo(1)–P(1)	2.4401(8)	2.4179(9)
Mo(2)–P(1)	2.4122(8)	2.378(1)
Mo(1)–S(1)	2.5360(9)	2.551(1)
Mo(1)–C(18)	1.951(4)	1.959(4)
Mo(1)–C(19)	1.943(4)	1.963(4)
P(1)–S(1)	2.050(1)	2.046(1)
P(1)–C(1)	1.773(3)	1.781(3)
Mo(2)–C(1)	2.269(3)	2.260(3)
Mo(2)–C(2)	2.218(3)	2.220(4)
Mo(2)–C(3)	2.278(3)	2.272(3)
Mo(2)–C(4)	2.352(3)	2.329(4)
Mo(2)–N/O	2.287(3)	2.159(3)
C(5)–C(7)	1.484(5)	1.498(6)
C(7)–N/O	1.277(4)	1.235(5)
C(18)–Mo(1)–C(19)	76.7(2)	76.9(2)
P(1)–Mo(1)–C(18)	107.1(1)	102.9(1)
P(1)–Mo(1)–C(19)	82.6(1)	84.8(1)
P(1)–Mo(2)–N/O	84.54(7)	84.16(8)
C(7)–N/O–Mo(2)	110.9(2)	115.8(3)

Spectroscopic data in solution for compounds **6b-f** (Table 1 and Experimental section) are similar to each other and to those of **6a**, therefore indicating a close structural relationship in this family of complexes, in turn consistent with the structure of **6a** found in the solid-state, and the same applies to the selenophosphinidene complex **8**. The IR spectra of these complexes are almost identical to each other, and close to those of the parent neutral complexes of type **1** as expected, while their ^{31}P chemical shifts are closer to those of their cationic precursors. The presence of the aldimine ligand in these complexes is denoted by strongly deshielded ^1H and ^{13}C NMR diagnostic resonances at ca. 7.8 and 180 ppm respectively, and its tethering to the C^5 carbon of the cyclohexadiene ring is indicated by the significant shielding of the corresponding ^1H and ^{13}C NMR resonances, now found at ca. 1.1-1.8 ppm and 53 ppm, respectively. Spectroscopic data in solution for compound **10** are similar to those of compounds **6**, except for the imine resonances, now replaced by diagnostic ^1H and ^{13}C NMR

resonances of the aldehyde group at 9.42 and 215.7 ppm, respectively (cf. 9.89 and 214.1 ppm respectively in $[WCp(CO)_3(\kappa^1\text{-}OCHPh)](CF_3SO_3)$).[16]

Structural characterization of complexes 7 and 9

The molecular structure of the aminocarbene complex **7a** was briefly described in our preliminary report on these reactions (Figure 3),[4] and only a few comments are needed here. Overall, the structure is very similar to those of **6a** or **10** discussed above, except that the coordination sphere around the Mo2 atom now is completed by an aminocarbene group tethered to the C^5 atom of the η^4-bound cyclohexadiene ligand. The environment around the carbene C7 atom is planar trigonal as expected, but so it is the one around the N atom, then allowing for some π-bonding interaction between these atoms. Indeed, the C–N length of 1.314(9) Å is closer to the reference double-bond length (1.26 Å)[14] than to the value expected for a single N–C(sp^2) bond (1.44 Å),[18] thus indicating the presence of significant multiplicity in this bond. The corresponding π-bonding interaction of course is detrimental to the π-bonding component of the metal-carbene bond, and indeed the Mo2–C7 distance of 2.063(7) Å is longer than expected for a conventional CR_2 ligand (cf. 1.951(3) Å in $[MoCp(\kappa^1\text{-}CHtBu)(NO)(Py)]$),[19] but still falls on the short side of the range of 2.07-2.22 Å measured previously for low-valent Mo or W aminocarbene complexes bearing Cp ligands (cf. 2.141(12) Å in $[MoCpI(\kappa^1\text{-}C(CH_2)_3NMe)(CO)_2]$),[20] thus indicating a relatively strong metal-aminocarbene binding for complex **7a**.

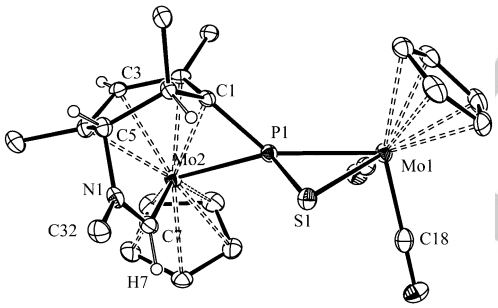

Figure 3. ORTEP diagram (30% probability) of compound **7a**, with most H atoms and *t*Bu groups (except their C^1 atoms) omitted for clarity. Selected bond lengths (Å): Mo(1)–P(1) = 2.440(2), Mo(2)–P(1) = 2.384(2), Mo(1)–S(1) = 2.5526(17), P(1)–S(1) = 2.049(2), Mo(2)–C(7) = 2.063(7), C(5)–N = 1.489(9), C(7)–N = 1.314(9). Selected bond angles: C(18)–Mo(1)–C(19) = 76.1(3), P(1)–Mo(1)–C(18) = 103.3(2), P(1)–Mo(1)–C(19) = 82.5(2), P(1)–Mo(2)–C(7)= 85.3(2).[4]

Spectroscopic data in solution for compounds **7b-d** (Table 1 and Experimental section) are similar to those of **7a** and consistent with the structure found in the solid-state for the latter, as it is the case of the selenophosphinidene complex **9**. Not surprisingly, most of these data also are very similar to those of the corresponding aldimine complexes of type **6** and **8**, and then deserve no particular comments. The significant difference, of course, is derived from the presence of aminocarbene ligands in compounds **7** and **9**, which give rise to highly deshielded ^1H and ^{13}C NMR diagnostic resonances at ca. 11 and 265 ppm respectively.

The intermediate species preceding complexes 6 and 7

As noted above, in our preliminary study we found that hydride attack on complex **2a** was initiated at a Cp ligand to give a cyclopentadiene intermediate then evolving to a hydride isomer in turn yielding the aldimine and aminocarbyne products eventually being isolated (Scheme 1).[4] We have now performed low-temperature NMR monitoring of the reactions of $K[BHsBu_3]$ with analogous complexes having *i*Pr (**2b**) and Xyl (**2e**) groups at the isocyanide ligand and found similar results, thus pointing to a quite general behavior for these cationic complexes (see the Experimental section). Upon mixing of the reagents at 213 K, an almost immediate reaction takes place to give in all cases the corresponding cyclopentadiene complex $[Mo_2Cp\{\mu\text{-}\kappa^2_{P,S}\text{:}\kappa^1_P,\eta^5\text{-}SP(C_6H_3{}^tBu_3)\}(\eta^4\text{-}C_5H_6)(CNR)(CO)_2]$ (**4**) as the unique product (Figure 4). These complexes evolve very slowly at this temperature, but rapidly at around 243 K, to yield the corresponding cyclopentadienyl hydride isomers $[Mo_2Cp_2\{\mu\text{-}\kappa^2_{P,S}\text{:}\kappa^1_P,\eta^3\text{-}SP(C_6H_3{}^tBu_3)\}(H)(CNR)(CO)_2]$ (**5**), a process following from the oxidative addition of a H–C(sp^3) bond of the cyclopentadiene ligand, and accompanied with a change in the hapticity of the C_6 ring of the phosphorus ligand (from η^5 to η^3) to balance the electron count at the Mo atom. However, this transformation is not complete, but reaches an equilibrium point, with the ratio **5**/**4** being ca. 5 in all cases at 243 K. A very minor isomer of **5** was also formed at this temperature in all cases, presumably having a cisoid arrangement of the Cp ligands relative to the central MoPS plane of these molecules (***cis*-5**, Figure 4). The equilibrium ratio between these hydride isomers were ca. 10 for the *t*Bu and Xyl compounds, and of ca. 15 in the case of **5b**. All these species, however, progressively disappeared from the corresponding solutions upon rising the temperature (rapidly at room temperature), to give the final mixture of compounds **6** and **7,** with no further intermediate species being detected, irrespective of the particular temperature chosen to follow this final stage.

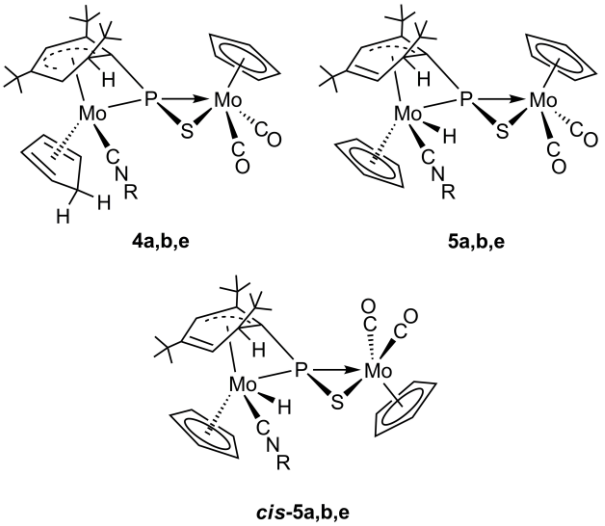

Figure 4. Structures of intermediate compounds **4** and **5**

Intermediates **4b,e** displayed spectroscopic data (see the Experimental Section) comparable to those of **4a**, in turn consistent with the DFT-optimized structure of the latter.[4] In particular, the ^{1}H and ^{13}C NMR resonances for the C_6 ring of the phosphorus ligand are comparable to those of the cationic precursors of type **2**, and one of the Cp resonances of the precursor has been replaced with NMR resonances characteristic of η^4-bound cyclopentadiene ligands,[21] while their number (six ^{1}H and five ^{13}C resonances) are consistent with the absence of symmetry elements in these molecules.

Spectroscopic data for intermediates **5b,e** also were comparable to those of the CN*t*Bu-intermediate **5a** identified in our preliminary investigation of this reaction. The salient spectroscopic features of these compounds of course are the recovery of the second Cp resonance and the appearance of a shielded ^{1}H NMR resonance at ca. –3.2 ppm corresponding to a terminal hydride, thus confirming the migration of a cyclopentadiene H atom to the metal site. The relatively large value of the corresponding coupling to the P nucleus (^{2}J(H,P) = 24-27 Hz) is consistent with the DFT-optimized structure of **5a**,[4] which displayed the hydride ligand placed between the P and C(N*t*Bu) atoms and defining a quite acute H–Mo–P angle of 62.4°.[22] As noted above, a very minor second hydride isomer was also detected in these reactions, it being characterized by similar ^{31}P and ^{1}H NMR resonances, therefore having similar coordination spheres around the metal atoms. In particular, the hydride resonance appeared at similar positions (ca. –2.60 ppm) and with only slightly higher P couplings (28-32 Hz), this ensuring that the relative positioning between the P and H nuclei is the same as it is in the major hydride isomer. Hence the hypothesis of a cisoid arrangement of the Cp ligands (relative to the MoPS plane) in these minor isomers. We note that such isomerism has been observed previously in several thiophosphinidene complexes related to compounds **1**, and it is actually present in the solid-state structure of **1a**.[9]

Reaction pathways in the formation of aldimine and aminocarbene derivatives of compounds 2 and 3

The experimental data discussed in the preceding sections indicate that the hydride attack on cations **2a-e** and **3**, as well as the subsequent evolution of the intermediates so formed, occurs in all cases in the same way as originally found for the CN*t*Bu complex **2a**. The nature of the isocyanide ligand, however, has a significant influence on the product distribution (i.e. the ratio between aldimine and aminocarbene derivatives). To better understand the elemental steps behind these intricate transformations we have first computed the whole kinetic pathway for the CN*t*Bu complex by starting from the corresponding cyclopentadiene intermediate **4a**. In a second stage, once identified the bifurcation point separating the aldimine and aminocarbene paths, we have computed these final steps for all other isocyanide complexes.

As for the fact that hydride attack occurs selectively at the Cp ligand of complexes **2** and **3**, we note that our calculations on complex **2a** indicate that the largest positive charge is localized at the P atom (see the Supporting Information), while the LUMO of the cation has a significant participation of the C^5 atom of the C_6 ring, which incidentally would be the preferred site for nucleophilic attack on the basis of the Davies-Green-Mingos rules.[5] However, the latter site is clearly disfavored on steric grounds, due to the presence of close *t*Bu groups. Then, by recalling that these reactions only proceed selectively when using relatively bulky hydride transfer reagents such as $[BHsBu_3]^-$ or $[BHEt_3]^-$, we are bound to conclude that the observed selectivity in the initial hydride attack on compounds **2** and **3** has a steric origin. We note here that a similar sterically-driven hydride attack at a coordinated Cp ligand was also observed for the quite congested phosphide-bridged cation $[(\eta^6\text{-}C_6H_3tBu_3)CpMo{-}P{\equiv}MoCp(CO)_2]^+$.[23]

Once the cyclopentadiene complex **4a** is formed, the reaction then proceeds to the C–H cleavage step *via* an agostic coordination of the *endo* C–H bond of the methylenic group, with simultaneous η^5 to η^3 slippage of the C_6 ring to keep the electron balance at the Mo atom (Figure 5). This occurs through an accessible transition state **TS1** (81 kJmol^{-1} above **4a**) to give an unstable agostic intermediate **A** (57 kJmol^{-1} above **4a**) which undergoes the oxidative addition of the agostic C–H bond in an almost barrierless way (*via* a transition state **TS2** placed just 1 kJmol^{-1} above **A**), to yield the cyclopentadienyl hydride intermediate **5a**. The computed energy for the latter species is only 2 kJmol^{-1} higher than **4a**, which is consistent with the experimental observation that an equilibrium between these two species is reached above ca. 243 K, although the right relative order (**5a** more stable than **4a** in THF solution) is not reproduced at this level of theory. Intermediate **5a** then evolves *via* migratory insertion of the isocyanide ligand into the Mo–H bond to yield a formimidoyl intermediate **B** of similar energy (only 9 kJmol^{-1} above **5a**). The latter is a well-known type of reaction for organometallic isocyanide complexes of any nuclearity.[24,25] In our case, this insertion is accompanied by a change in the hapticity of the C_6 ring (from η^3 back to the η^5 mode) in order to keep the electron count at the Mo atom, and it is the rate-determinant step, since the corresponding transition state **TS3** has the highest energy. Moreover, since **TS3** is placed ca. 90 kJmol^{-1} above **5a**, it can be predicted that the rearrangement of **5a** into **B** would be very slow at around 243 K, but reasonably fast at room temperature, in agreement with our experimental observations. Finally we realize that, since the transition states connecting **B** to the final products **6** and **7** are of lower energy (see below), then it is not surprising that we failed to observe significant amounts of this intermediate at any temperature.

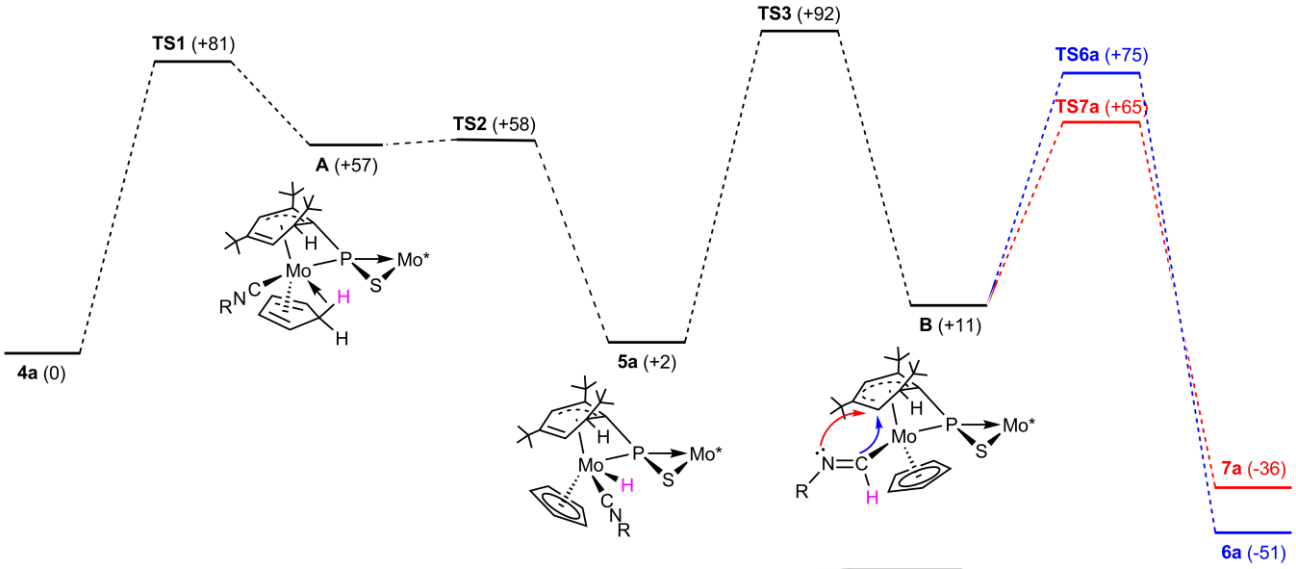

Figure 5. DFT-B3LYP computed kinetic profile for the rearrangement of intermediate **4a** into complexes **6a** and **7a** in tetrahydrofuran solution, with their relative Gibbs free energies at 298 K (in kJmol^{-1}) indicated between brackets (Mo* = MoCp(CO)$_2$; R = *t*Bu).

The formimidoyl intermediate **B** actually represents the bifurcation point in this reaction, since it can further evolve in two different ways. As a first option, the N atom of the iminoacyl ligand may just perform a nucleophilic attack at the C^5 atom of the C$_6$ ring to give the aminocarbene complex **7a**. This requires a minimum geometrical reorganization (rotation around the Mo–C bond so the NR group approaches the C$_6$ ring) and thus proceeds *via* the less energetic transition state **TS7a**, placed only 54 kJmol^{-1} above **B**. As a second option, the formimidoyl ligand may alternatively undergo migratory insertion into the Mo–C^5 bond of the η^5-coordinated ring, itself an unprecedented event as noted at the Introduction section. Moreover, this rearrangement also requires the simultaneous approach of the N atom to the metal site to eventually yield the aldimine derivative **6a**. Thus, perhaps it is not surprising that this complex rearrangement proceeds *via* a more energetic transition state **TS6a** (10 kJmol^{-1} above **TS7a**), even if the final aldimine complex **6a** is 15 kJmol^{-1} more stable than the carbene isomer **7a**, therefore being the thermodynamic product in this reaction. Correspondingly, the aminocarbene complex **7a** is identified as the kinetic product. We must remark that the insertion of C-based ligands into M–C bonds of η-bound hydrocarbyl ligands are extremely rare reactions in general. We can quote a few precedents of insertions into transition metal-indenyl bonds (e.g. benzophenone into [Zr(η^5-indenyl)(η^9-indenyl)]),[26] while some heterocumulenes have been found also to insert into the metal-cyclopentadienyl bond of the lanthanide complex YCp$_3$.[7] Apparently these insertion reactions relay on the haptotropic flexibility of the η-bound ligands in these substrates (even down to the η^1 mode), a circumstance not required in the case of intermediate **B**.

Table 3. DFT-computed energies for key precursors of compounds **6** and **7**[a]

R	Xyl	*t*Bu	*i*Pr	Ph	Ph'	H
TS6	70	64	61	55	50	56
TS7	102	54	51	46	45	45
6	–33	–62	–73	–87	–89	–126
7	+16	–47	–50	–57	–56	–88
Therm. pref. **6**[b]	+49	+15	+23	+30	+33	+38
Kinetic pref. **6**[c]	+32	–10	–10	–9	–5	–11
Mo–N in **6** (Å)	2.428	2.363	2.313	2.264	2.263	2.166
Exp. ratio **6**/**7**	>>>	0.4	0.25	1.3	2.2	

[a] Gibbs free energies (in kJmol^{-1}) in tetrahydrofuran solution at 298 K, relative to the corresponding intermediate species of type **B**; Ph' = 4-C$_6$H$_4$OMe. [b] The thermodynamic preference for **6** is estimated as the energy difference **7**-**6**. [c] The kinetic preference for **6** is estimated as the energy difference **TS7**-**TS6**

We have also computed the transformations **B**/**6** and **B**/**7** for all other isocyanide complexes used in this work, as well as the corresponding hypothetical species having a CNH ligand (see the SI). Similar transition states of the types **TS6** and **TS7** were found in all cases, and the computed energies (relative to the corresponding intermediates of type **B**) are collected in Table 3.[27] From the analysis of all these data we can extract some general trends. Firstly, we note that the aldimine complexes **6** are the thermodynamic products in all cases, with energetic preference in the range 15-50 kJmol^{-1}, while formation of the aminocarbene isomers **7** involves kinetic barriers some 10 kJmol^{-1} lower in general (except for R = Xyl), thus explaining the formation of both **6** and **7** in most cases. Secondly, the bulkiness of the R group of the isocyanide ligand (Xyl > *t*Bu > *i*Pr > Ph ≈ 4-C$_6$H$_4$OMe >> H) seems to be a most critical factor in the

thermodynamics of these reactions; it has a progressive de-stabilizing effect on both **6** and **7**, but more pronounced for the aldimine complexes **6** (particularly reflected in the progressive increase of the Mo–N lengths from H to Xyl, see Table 3), thus justifying the prevalence of the aminocarbene products **7** for the bulkier *t*Bu and *i*Pr groups; this thermodynamic influence is further confirmed by the fact that the maximum stability relative to **B** is reached when R = H. In the third place, we note that an opposite influence is found for the very bulky Xyl group, which has a particularly strong de-stabilizing effect on both the hypothetical carbene product **7e** (16 kJmol^{-1} above **B**) and the corresponding transition state (102 kJmol^{-1} above **B**), thus explaining why only the aldimine **6e** is formed in this case. Some of this influence might be already present at the *t*Bu system, since the relative amount of the carbene product in this case is somewhat lower (rather than higher) than the one obtained for the less crowded *i*Pr system. Finally, even if electronic effects are difficult to separate from steric ones, the data for R = Ph and 4-C_6H_4OMe (same steric influence) suggest that electron-withdrawing groups might favor to some extent the formation of aldimine complexes **6**, both on the thermodynamic and kinetic sizes; as a corollary, the electron-donor groups *t*Bu and *i*Pr would somewhat favor the formation of the aminocarbene complexes **7**, in line with the steric influence of these groups

Conclusions

The unusual C–C and C–N couplings first unveiled upon hydride attack on the *t*Bu isocyanide complex **2a** have now proven to be general processes occurring for other isocyanide complexes. The reaction initiates in all cases by hydride attack on the Cp ligand to give a cyclopentadiene intermediate. This is not the favored site of nucleophilic attack on either charge or orbital grounds, but rather a less hindered site on steric grounds. This first intermediate then undergoes the cleavage of one of the methylene C–H bonds to give a cyclopentadienyl hydride intermediate of similar energy. Since the kinetic barriers involved in this transformation are relatively low, then equilibrium between these two intermediates can be reached at low temperature. At room temperature, however, the hydride intermediate undergoes migratory insertion of the isocyanide ligand into the Mo–H (the rate-limiting step of the overall process) to yield a formimidoyl intermediate (not observed). All these processes are facilitated by the haptotropic flexibility of the cyclohexadienyl substituent at the P atom, which switches its binding to the Mo atom from η^5- to η^3- and then back to the η^5-mode, thus accommodating the coordinative and electronic changes derived from the long H-shift from Cp up to the CNR ligand. The formimidoyl intermediate then can evolve in two competitive ways: either *via* a nucleophilic attack of the N(formimidoyl) atom to the cyclohexadienyl ring (C–N coupling) that yields the aminocarbene product, or *via* insertion of the formimidoyl ligand into the Mo–η^5-hexadienyl bond (C–C coupling) to give the more stable aldimine isomer. The kinetic barrier for the first process is some 10 kJmol^{-1} lower in general, thus explaining the formation of both products in most cases, and the bulkiness of the R group of the isocyanide ligand has a stronger de-stabilizing effect on the aldimine complexes, then favoring the prevalence of the aminocarbene products in the final mixture. However, the very bulky Xyl group has a particularly strong de-stabilizing effect on the carbene product, which is not formed at all in that case.

Experimental Section

General Procedures and Starting Materials

All manipulations and reactions were carried out under an argon (99.995%) atmosphere using standard Schlenk techniques. All experiments were carried out using Schlenk tubes equipped with Young´s valves. Solvents were purified according to literature procedures and distilled prior to use.[28] Petroleum ether refers to that fraction distilling in the range 338-343 K. Compounds $[Mo_2Cp_2(\mu\text{-}\kappa^1\text{:}\kappa^1,\eta^6\text{-PMes*})(CO)_2]$ (**I**),[29] **1a** and $[Mo_2Cp_2(\mu\text{-}\kappa^2_{P,Se}\text{:}\kappa^1_P,\eta^4\text{-SePMes*})(CO)_2(CN\textit{t}Bu)]$,[9] **2a**,[10] and $[H(OEt_2)_2](BAr'_4)$,[30] were prepared as described previously (Mes* = 2,4,6-C_6H_2*t*Bu$_3$; Ar´= 3,5-$C_6H_3(CF_3)_2$), while all other reagents were obtained from the usual commercial suppliers and used as received, unless otherwise stated. Chromatographic separations were carried out using jacketed columns cooled by tap water (ca. 288 K) or by a closed 2-propanol circuit, kept at the desired temperature with a cryostat. Commercial aluminum oxide (activity I, 70-290 mesh) was degassed under vacuum prior to use. The latter was mixed under argon with the appropriate amount of water to reach activity IV. IR stretching frequencies were measured in solution, are referred to as ν(bond) and given in wave numbers (cm^{-1}). Nuclear magnetic resonance (NMR) spectra were routinely recorded in CD_2Cl_2 solutions at 293 K unless otherwise stated. Chemical shifts (δ) are given in ppm, relative to internal tetramethylsilane (^{1}H, ^{13}C) or external 85% aqueous H_3PO_4 (^{31}P). Coupling constants (J) are given in Hz.

Preparation of *syn*-$[Mo_2Cp_2(\mu\text{-}\kappa^2_{P,S}\text{:}\kappa^1_P,\eta^4\text{-SPMes*})(CN\textit{i}Pr)(CO)_2]$ (1b). A dichloromethane solution of S_8 (1 mL of a 0.081 M solution, 0.081 mmol) and neat CN*i*Pr (8 μL, 0.085 mmol) were added to a dichloromethane solution (5 mL) of compound **I** (0.050 g, 0.076 mmol), and the mixture was stirred at room temperature for 2 h to give an orange solution. After removal of the solvent under vacuum, the residue was extracted with dichloromethane/petroleum ether (1/4) and the extracts were chromatographed on alumina. Elution with dichloromethane/petroleum ether (1/1) gave an orange fraction yielding, after removal of solvents, compound **1b** as an orange microcrystalline solid (0.055 g, 95%). ^{1}H NMR (300.13 MHz, CD_2Cl_2): δ = 5.95 (s, 1H, C_6H_2), 5.52 (d, J(H,P) = 5, 1H, C_6H_2), 5.40 (s, 5H, Cp), 5.02 (d, J(H,P) = 2, 5H, Cp), 4.26 [septet, J(H,H) = 7, 1H, CH(*i*Pr)], 1.46, 1.43 [2d, J(H,H) = 7, 2 x 3H, CH_3(*i*Pr)], 1.39, 1.02, 0.99 (3s, 3 x 9H, *t*Bu); ^{13}C{^{1}H} NMR (75.47 MHz, CD_2Cl_2): δ =257.2 (d, J(C,P) = 27, MoCO), 244.2 (s, MoCO), 151.9 [s, $C^6(C_6H_2)$], 133.1 [d, J(C,P) = 2, $C^5(C_6H_2)$], 99.4 [d, J(C,P) = 13, $C^2(C_6H_2)$], 96.3 [d, J(C,P) = 1, $C^4(C_6H_2)$], 93.0, 89.2 (2s, Cp), 84.3 [d, J(C,P) = 6, $C^3(C_6H_2)$], 61.6 [d, J(C,P) = 35, $C^1(C_6H_2)$], 49.8 [s, C^1(*i*Pr)], 39.4, 35.3, 35.2 [3s, C^1(*t*Bu)], 34.0, 32.8, 31.6 [3s, C^2(*t*Bu)], 23.5, 23.2 [2s, C^2(*i*Pr)]; the resonance of the Mo-bound C atom of the isocyanide ligand could not be located in this spectrum; labeling of the ring C atoms according to the scheme shown below; elemental analysis calcd(%) for $C_{34}H_{46}Mo_2NO_2PS$: C 54.04, H 6.14, N 1.85, S 4.24; found: C 54.22, 6.11, N 1.80, S 4.12.

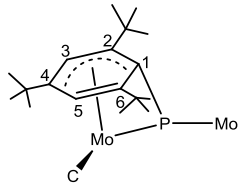

Preparation of compounds 1c-e. The procedure is analogous to the one described for **1b**, see the Supporting Information.

Preparation of [$Mo_2Cp_2\{\mu$-$\kappa^2_{P,S}$:κ^1_P,η^5-$SP(C_6H_3tBu_3)\}(CNiPr)(CO)_2$](BAr´$_4$) (2b). Solid [H($OEt_2$)$_2$](BAr´$_4$) (0.075 g, 0.074 mmol) was added to a dichloromethane solution (4 mL) of compound **1b** (0.055 g, 0.073 mmol) at 213 K, and the mixture was stirred for 1 min to give a red-brown solution which was chromatographed on an alumina column packed in dichloromethane (activity IV) at 285 K. Elution with dichloromethane gave a reddish band yielding, after removal of the solvent under vacuum, compound **2b** as a brown microcrystalline solid (0.112 g, 95%). ^{1}H NMR (300.13 MHz, CD_2Cl_2): δ = 7.74 (m, 8H, Ar´), 7.58 (s, 4H, Ar´), 6.26 (dd, J(H,P) = 4, J(H,H) = 2, 1H, C_6H_3), 5.50 (s, 5H, Cp), 5.48 (d, J(H,P) = 1, 5H, Cp), 5.05 (dd, J(H,H)= 6, 2, 1H, C_6H_3), 4.31 [septet of d, J(H,H) = 7, J(H,P) = 1, 1H, CH(*i*Pr)], 3.63 (dd, J(H,P) = 10, J(H,H) = 6, 1H, C_6H_3), 1.53,1.49 [2d, J(H,H) = 7, 2 x 3H, CH_3(*i*Pr)], 1.28, 1.21, 0.77 (3s, 3 x 9H, *t*Bu); ^{13}C{^{1}H} NMR (75.47 MHz, CD_2Cl_2): δ = 254.6 (d, J(C,P) = 26, MoCO), 236.6 (s, MoCO), 162.2 [m, J(C,B) = 49, C^1(Ar´)], 153.7 (s, br, MoCN), 135.3 [s, C^2(Ar´)], 129.4 [qm, J(C,F) = 32, J(C,B) = 3, C^3(Ar´)], 125.1 (q, J(C,F) = 272, CF_3), 124.8 [s, C^4(C_6H_3)], 119.0 [d, J(C,P) = 11, C^2(C_6H_3)], 118.0 [m, C^4(Ar´)], 95.1, 92.7 (2s, Cp), 89.7 [d, J(C,P) = 9, C^5(C_6H_3)], 88.9 [d, J(C,P) = 4, C^3(C_6H_3)], 58.2 [s, C^6(C_6H_3)], 54.6 [d, J(C,P) = 44, C^1(C_6H_3)], 52.9 [s, C^1(*i*Pr)], 40.6, 40.3, 36.0 [3s, C^1(*t*Bu)], 34.6 [d, J(C,P) = 2, C^2(*t*Bu)], 31.2, 25.5 [2s, C^2(*t*Bu)], 22.4 [s, 2C^2(*i*Pr)]; labeling of the ring C atoms according to the scheme shown below; elemental analysis calcd (%) $C_{66}H_{59}BF_{24}Mo_2NO_2PS$: C 48.94, H 3.67, N 0.86, S 1.98; found: C 49.01, H 3.75, N 0.90, S 1.85.

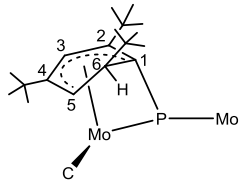

Preparation of compounds 2c-e. The procedure is analogous to the one described for **2b**, see the Supporting Information.

Preparation of [$Mo_2Cp_2\{\mu$-$\kappa^2_{P,Se}$:κ^1_P,η^5-$SeP(C_6H_3tBu_3)\}(CNtBu)(CO)_2$](BAr´$_4$) (3). Solid [H($OEt_2$)$_2$](BAr´$_4$) (0.050 g, 0.049 mmol) was added to a dichloromethane solution (4 mL) of compound [Mo_2Cp_2(μ-$\kappa^2_{P,Se}$:κ^1_P,η^4-SePMes*)$(CO)_2$($CNtBu$)] (0.040 g, 0.049 mmol) at 213 K, and the mixture was stirred for 1 min to give a red-brown solution which was chromatographed on an alumina column packed in dichloromethane (activity IV) at 285 K. Elution with dichloromethane gave a reddish band yielding, after removal of the solvent under vacuum, compound **3** as a brown-orange microcrystalline solid (0.077 g, 94%). ^{1}H NMR (300.13 MHz, CD_2Cl_2): δ = 7.73 (m, 8H, Ar´), 7.58 (s, 4H, Ar´), 6.26 (dd, J(H,P) = 4, J(H,H) = 2, 1H, C_6H_3), 5.49 (d, J(H,P) = 1, 5H, Cp), 5.47 (s, 5H, Cp), 5.02 (dd, J(H,H) = 7, J(H,P) = 2, 1H, C_6H_3), 3.67 (dd, J(H,P) = 10, J(H,H) = 7, 1H, C_6H_3), 1.59, 1.28, 1.22, 0.78 (4s, 4 x 9H, *t*Bu); elemental analysis calcd (%) for $C_{67}H_{61}BF_{24}Mo_2NO_2PSe$: C 47.88, H 3.66, N 0.83; found: C 47.62, H 3.44, N 0.82.

NMR monitoring of the reaction of compound 2b with K[$BHsBu_3$]: Identification of the intermediate complexes [$Mo_2Cp\{\mu$-$\kappa^2_{P,S}$:κ^1_P,η^5-$SP(C_6H_3tBu_3)\}(\eta^4$-$C_5H_6)(CNiPr)(CO)_2$] (4b) and [$Mo_2Cp_2\{\mu$-$\kappa^2_{P,S}$:κ^1_P,η^3-$SP(C_6H_3tBu_3)\}(H)(CNiPr)(CO)_2$] (5b). A THF-$d_8$ solution (0.5 mL) of compound **2b** (0.050 g, 0.031 mmol) was placed in an NMR tube equipped with a Young´s valve and cooled at 213 K. Then K[$BHsBu_3$] (30 μL of a 1.0 M solution in THF, 0.030 mmol) was added to the solution, and the mixture was monitored by NMR starting at 213 K. Both the ^{31}P{^{1}H} and ^{1}H NMR spectra recorded after 2 min at that temperature revealed the presence of a single species, identified as the cyclopentadiene complex **4b**, and after 3.5 h at 213 K an equilibrium mixture of isomers **4b**/***trans*-5b** (1/5) was reached (in a few min at 233 K). A small amount of ***cis*-5b** was also present (1/15 relative to its *trans* isomer at 233 K). Upon raising the temperature up to 293 K, the final mixture **6b**/**7b** (1/2) was obtained after 20 min. *Data for* ***4b***: ^{1}H NMR (400.13 MHz, THF-d_8, 213 K): δ = 5.85 (d, br, J(H,P) = 4, 1H, C_6H_3), 5.46 (s, br, 1H, C_5H_6), 5.37 (s, 5H, Cp), 5.25 (s, br, 1H, C_5H_6), 4.32 [septet, J(H,H) = 7, 1H, CH(*i*Pr)], 4.11 (d, J(H,H) = 6, 1H, C_6H_3), 3.81 (dd, J(H,P)= 9, J(H,H)= 6, 1H, C_6H_3), 2.97, 2.73 [2d, J(H,H) = 9, 2 x 1H, $CH_2(C_5H_6)$], 2.62 (d, J(H,P) = 9, 1H, C_5H_6), 2.53 (s, br, 1H, C_5H_6), 1.56, 1.51 [2d, J(H,H) = 7, 2 x 3H, CH_3(*i*Pr)], 1.22, 1.10, 0.70 (3s, 3 x 9H, *t*Bu). ^{31}P{^{1}H} NMR (161.99 MHz, THF-d_8, 213 K): δ = 113.4 (s). *Data for* ***trans-5b*** (major isomer): ^{1}H NMR (400.13 MHz, THF-d_8, 233 K): δ = 5.47, 5.45 (2s, 2 x 5H, Cp), 4.78 (d, J(H,P) = 2, 1H, C_6H_3), 4.09 [septet, J(H,H) = 6, 1H, CH(*i*Pr)], 3.27 (d, J(H,P) = 4, 1H, C_6H_3), 2.21 (dd, J(H,P) = 11, J(H,H) = 4, 1H, C_6H_3), 1.35, 1.33 [2d, J(H,H)= 6, 2 x 3H, CH_3(*i*Pr)], 1.24, 1.18, 0.99 (3s, 3 x 9H, *t*Bu), –3.37 (d, J(H,P) = 27, 1H, MoH); ^{31}P{^{1}H} NMR (161.99 MHz, THF-d_8, 233 K): δ = 87.4 (s). *Data for* ***cis-5b*** (minor isomer)*:* ^{1}H NMR (400.13 MHz, THF-d_8, 233 K): δ = –2.70 (d, J(H,P) = 32, 1H, MoH); ^{31}P{^{1}H} NMR (161.99 MHz, THF-d_8, 233 K): δ = 75.7 (s).

NMR monitoring of the reaction of compound 2e with K[$BHsBu_3$]. The procedure is analogous to the one described for **2b**, see the Supporting Information.

Preparation of [$Mo_2Cp_2\{\mu$-$\kappa^2_{P,S}$:$\kappa^2_{P,N}$,η^4-$SP(C_6H_3tBu_3(CHNiPr))\}(CO)_2$] (6b) and [$Mo_2Cp_2\{\mu$-$\kappa^2_{P,S}$:$\kappa^2_{P,C}$,$\eta^4$-$SP(C_6H_3tBu_3(NiPrCH))\}(CO)_2$] (7b). A solution of K[$BHsBu_3$] (K-selectride) (75 μL of a 1.0 M solution in THF, 0.075 mmol) was added to a tetrahydrofuran solution (6 mL) of compound **2b** (0.116 g, 0.072 mmol) at 213 K, and the mixture was stirred for 1 min, then allowed to reach room temperature and further stirred for 20 min to give an orange solution. The solvent was then removed under vacuum, the residue was extracted with dichloromethane/petroleum ether (1/4) and the extracts were chromatographed on an alumina column (activity IV) at 285 K. Elution with dichloromethane/petroleum ether (1/4) gave a dark orange fraction yielding, after removal of solvents, compound **6b** as an orange microcrystalline solid (0.008 g, 15%). Elution with dichloromethane/petroleum ether (1/2) gave another orange fraction yielding analogously compound **7b** as an orange microcrystalline solid (0.042 g, 77%). *Data for compound* ***6b***: ^{1}H NMR (400.13 MHz, CD_2Cl_2): δ = 7.76 (d, J(H,H) = 3, 1H, CHN), 5.40 (d, J(H,P) = 10, 1H, C_6H_3), 5.39 (s, 5H, Cp), 5.08 (d, J(H,P) = 2, 5H, Cp), 3.71 (dd, J(H,H) = J(H,P) = 3, 1H, C_6H_3), 3.29 [septet, J(H,H) = 7, 1H, CH(*i*Pr)], 1.45 (d, J(H,H) = 7, 3H, CH_3), 1.20 (s, 9H, *t*Bu), 1.12 (d, J(H,H) = 7, 3H, CH_3), 1.10 (d, J(H,P) = 7, 1H, C_6H_3), 1.02, 0.97 (2s, 2 x 9H, *t*Bu); ^{13}C{^{1}H} NMR (75.47 MHz, CD_2Cl_2): δ = 257.4 (d, J(C,P) = 28, MoCO), 244.7 (s, MoCO), 173.8 (s, CHN), 107.2 [s, C^2(C_6H_3)], 93.5 (s, Cp), 92.1 [d, J(C,P) = 13, C^4(C_6H_3)], 91.9 [d, J(C,P) = 10, C^3(C_6H_3)], 90.1 (s, Cp), 61.9 [s, C^1(N*t*Bu)], 52.8 [d, J(C,P) = 34, C^1(C_6H_3)], 52.7 [s, C^5(C_6H_3)], 42.9 [s, C^6(C_6H_3)], 39.8, 37.0, 35.1 [3s, C^1(*t*Bu)], 33.9, 31.3 [2s, C^2(*t*Bu)], 29.2 [s, br, C^2(*t*Bu)], 24.8, 23.8 [2s, CH_3]; labeling of the ring C atoms according to the scheme shown below; elemental analysis calcd (%) for $C_{34}H_{48}Mo_2NO_2PS$: C 53.90, H 6.39, N 1.85, S 4.23; found: C 54.02, H 6.58, N 1.94, S 4.01.

Data for compound ***7b***: ^{1}H NMR (300.13 MHz, CD_2Cl_2): δ = 10.99 (dd, J(H,H) = J(H,P) = 2, 1H, CHN), 5.38 (d, J(H,P) = 11, 1H, C_6H_3), 5.33 (s, 5H, Cp), 5.28 (d, J(H,P) = 2, 5H, Cp), 4.85 (s, br, 1H, C_6H_3), 3.85 [septet, J(H,H) = 7, 1H, CH(*i*Pr)], 1.42 (d, J(H,H) = 7, 3H, CH_3), 1.39 (d, J(H,P) = 7,

1H, C_6H_3), 1.35 (d, *J*(H,H) = 7, 3H, CH_3), 1.27, 1.01, 0.98 (3s, 3 x 9H, *t*Bu); $^{13}C\{^1H\}$ NMR (75.47 MHz, CD_2Cl_2): δ = 257.7 (d, *J*(C,P) = 10, MoCHN), 256.8 (d, *J*(C,P) = 27, MoCO), 244.5 (s, MoCO), 105.2 [s, $C^2(C_6H_3)$], 95.5 [d, *J*(C,P) = 12, $C^4(C_6H_3)$], 93.4 (s, Cp), 91.8 [d, *J*(C,P) = 10, $C^3(C_6H_3)$], 91.4 (s, Cp), 77.7 [s, $C^5(C_6H_3)$], 55.9 [s, CH(*i*Pr)], 53.5 [d, *J*(C,P) = 33, $C^1(C_6H_3)$], 45.8 [s, $C^6(C_6H_3)$], 38.0, 36.8, 34.6 [3s, C^1(*t*Bu)], 34.0, 32.0, 29.6 [3s, C^2(*t*Bu)], 22.6, 22.4 (2s, CH_3); elemental analysis calcd (%) for $C_{34}H_{48}Mo_2NO_2PS$: C 53.90, H 6.39, N 1.85, S 4.23; found: C 54.13, H 6.42, N 1.76, S 4.05.

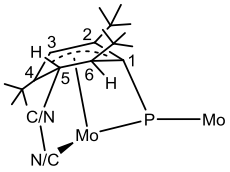

Preparation of compounds 6c-e, 7c,d, 8 and 9. The procedure is analogous to the one described for compounds **6b** and **7b**, see the Supporting Information.

Preparation of $[Mo_2Cp_2\{\mu\text{-}\kappa^2_{P,S}\text{:}\kappa^2_{P,N},\eta^4\text{-}SP(C_6H_3tBu_3(CHNnBu))\}(CO)_2]$ (6f). Net NH_2nBu (20 μL, 0.202 mmol) and excess molecular sieves (ca. 1 g) were added to a dichloromethane solution (4 mL) of compound **10** (0.015 g, 0.021 mmol), and the mixture was stirred at room temperature for 60 h to give a red-orange solution. The solvent was then removed under vacuum, the residue was extracted with dichloromethane/petroleum ether (1/4) and the extracts were chromatographed on an alumina column (activity IV) at 285 K. Elution with the same solvent mixture gave an orange-salmon fraction yielding, after removal of solvents, compound **6f** as a red-orange microcrystalline solid (0.012 g, 74%). ^1H NMR (300.13 MHz, CD_2Cl_2): δ = 7.57 (s, br, 1H, NCH), 5.39 (s, 5H, Cp), 5.09 (d, *J*(H,P) = 2, 5H, Cp), 3.73 (dd, *J*(H,H) = *J*(H,P) = 2, 1H, C_6H_3), 3.43, 2.96 (2m, 2 x 1H, NCH_2), 1.70-1.25 (m, 4H, CH_2), 1.14 (d, *J*(H,P) = 7, 1H, C_6H_3), 1.21, 1.18, 1.07 (3s, 3 x 9H, *t*Bu), 0.92 (t, *J*(H,H) = 7, 3H, CH_3); one of the proton resonances of the C_6H_3 ring could not be clearly identified in the spectrum; $^{13}C\{^1H\}$ NMR (75.47 MHz, CD_2Cl_2): δ = 257.2 (d, *J*(C,P) = 28, MoCO), 244.4 (s, MoCO), 176.8 (s, NCH), 107.2 [s, $C^2(C_6H_3)$], 93.5 (s, Cp), 92.6 [d, *J*(C,P) = 12, $C^4(C_6H_3)$], 91.7 [d, *J*(C,P) = 10, $C^3(C_6H_3)$], 90.4 (s, Cp), 65.1 [s, C^1(Bu)], 53.2 [s, $C^5(C_6H_3)$], 42.2 [s, $C^6(C_6H_3)$], 39.6, 37.0, 35.1 [3s, C^1(*t*Bu)], 33.8, 31.2 [2s, C^2(*t*Bu)], 33.0 [s, C^2(*n*Bu)], 29.2 [s, br, C^1(*t*Bu)], 20.7 [s, C^3(*n*Bu)], 14.2 [s, C^4(*n*Bu)]; the resonance for the C^1 atom of the C_6H_3 ring could not be clearly identified in the spectrum; elemental analysis calcd (%) for $C_{34}H_{48}Mo_2NO_2PS$: C 54.47, H 6.53, N 1.82, S 4.16; found: C 54.22, H 5.99, N 1.71, S 4.03.

Preparation of $[Mo_2Cp_2\{\mu\text{-}\kappa^2_{P,S}\text{:}\kappa^2_{P,O},\eta^4\text{-}SP(C_6H_3tBu_3(CHO))\}(CO)_2]$ (10). Solid benzoic acid (0.001 g, 0.008 mmol) and excess degassed water (50 μL, 0.202 mmol) were added to a dichloromethane solution (4 mL) of compound **6e** (0.038 g, 0.046 mmol), and the mixture was stirred at room temperature for 24 h to give an orange solution. The solvent was then removed under vacuum, the residue was extracted with dichloromethane/petroleum ether (1/2) and the extracts were chromatographed on an alumina column (activity IV) at 253 K. Elution with dichloromethane/petroleum ether (2/1) gave an orange fraction yielding, after removal of solvents, compound **10** as an orange microcrystalline solid (0.027 g, 81%). The crystals used in the X-ray diffraction study were grown by the slow diffusion of layers of toluene and petroleum ether into a concentrated dichloromethane solution of the complex at 253 K. ^1H NMR (400.13 MHz, CD_2Cl_2): δ = 9.42 (s, 1H, HCO), 5.63 [d, *J*(H,P) = 10, 1H, C_6H_3), 5.41 (s, 5H, Cp), 5.22 (d, *J*(H,P) = 2, 5H, Cp), 4.03 (s, br, 1H, C_6H_3), 1.41 (d, *J*(H,P) = 7, 1H, C_6H_3), 1.12, 1.03, 1.01 (3s, 3 x 9H, *t*Bu); $^{13}C\{^1H\}$ NMR (100.63 MHz, CD_2Cl_2): δ = 256.3 (d, *J*(C,P) = 29, MoCO), 242.9 (s, MoCO), 215.7 (s, HCO), 108.6 [s, $C^2(C_6H_3)$], 95.8 [d, *J*(C,P) = 12, $C^4(C_6H_3)$], 93.6 [d, *J*(C,P) = 10, $C^3(C_6H_3)$], 93.5, 91.7 (2s, Cp), 58.4 [s, $C^5(C_6H_3)$], 53.2 [d, *J*(C,P) = 34, $C^1(C_6H_3)$], 39.3 [s, C^1(*t*Bu)], 39.0 [s, $C^6(C_6H_3)$], 36.6, 35.8 [2s, C^1(*t*Bu)], 33.6, 30.4 [2s, C^2(*t*Bu)], 29.0 [s, br, C^2(*t*Bu)]; elemental analysis calcd (%) for $C_{31}H_{41}Mo_2O_3PS$: C 51.96, H 5.77, S 4.47; found: C, 51.61, H, 5.62, S 4.23.

X-ray Structure Determination of Compound 10

Data collection was performed at 123 K on an Oxford Diffraction Xcalibur Nova single crystal diffractometer, using Cu Kα radiation. Images were collected at a 63 mm fixed crystal-detector distance, using the oscillation method, with 1º oscillation and variable exposure time per image (1.5-3.9 s). Data collection strategy was calculated with the program *CrysAlis Pro CCD*,[31] and data reduction and cell refinement was performed with the program *CrysAlis Pro RED*.[31] An empirical absorption correction was applied using the SCALE3 ABSPACK algorithm as implemented in the latter program. Using the program suite *WINGX*,[32] the structure was solved by Patterson interpretation and phase expansion using *SHELXL2016*,[33] and refined with full-matrix least squares on F^2 using *SHELXL2016*. All non-hydrogen atoms were refined anisotropically, and all hydrogen atoms were geometrically placed and refined using a riding model, except for H(3), H(5), H(6) and H(7), which were located on the Fourier maps and refined riding on their parent atoms.

Computational Details

All DFT computations were carried out using the GAUSSIAN03 package,[34] in which the hybrid method B3LYP was used with the Becke three-parameter exchange functional[35] and the Lee-Yang-Parr correlation functional.[36] An accurate numerical integration grid (99,590) was used for all the calculations via the keyword Int=Ultrafine. Effective core potentials and their associated double-ζ LANL2DZ basis set were used for the metal atoms.[37] The light elements (P, S, O, C, N and H) were described with the 6-31G* basis.[38] Geometry optimizations were performed under no symmetry restrictions using initial coordinates derived from X-ray data, and frequency analyses were performed for all the stationary points to ensure that minimum structures with no imaginary frequencies (intermediates and products) or just one (transition states) were achieved. Their connectivity was corroborated through Intrinsic-Reaction-Coordinate (IRC) calculations. Solvent effects (THF, ε = 7.4257) were modeled using the polarized-continuum-model of Tomasi and co-workers (PCM),[39] by using the gas-phase optimized structures.

Supporting Information

A CIF file containing full crystallographic data for compound **10** (CCDC 1558433), a PDF file containing full preparative and spectroscopic data for all new compounds, results of DFT calculations (drawings, atomic coordinates and energies), crystal data for **10** and the complete reference 34, and an XYZ file including the Cartesian coordinates for all computed species.

Acknowledgements

We thank the Universidad de Oviedo for a grant (to B.A.), its CMC for access to computing facilities and its X-ray diffraction service for the acquisition of the diffraction data. We also thank the Gobierno del Principado de Asturias (Project GRUPIN14-011) and the MINECO of Spain and FEDER (Project CTQ2015-63726-P) for financial support.

Keywords: C–H activation • carbene ligands • imine ligands • C–C coupling • C–N coupling

[1] a) J. P. Collman, L. S. Hegedus, J. R. Norton, R. G. Finke, *Principles and Applications of Organotransition Metal Chemistry*, University Science Books, Mill Valley, **1987**, Chapters 7 and 8. b) J. F. Hartwig, *Organotransition Metal Chemistry*, University Science Books, Mill Valley, **2010**, Chapters 11 and 12.

[2] a) M. Delferro, T. J. Marks, *Chem. Rev.* **2011**, *111*, 2450-2485; b) W.-H. Zhang, S. W. Chien, T. S. A. Hor, *Coord. Chem. Rev.* **2011**, *255*, 1991-2024; c) G. Erker, *Organometallics*, **2011**, *30*, 358-368; d) M. Bochmann, *Organometallics* **2010**, *29*, 4711-4740; e) A. Otero, J. Fernández-Baeza, A. Lara-Sánchez, J. Tejeda, L. F. Sánchez-Barba, *Eur. J. Inorg. Chem.* **2008**, 5309-5326.

[3] a) B. Askevold, H. W. Roesky, S. Schneider, *ChemCatChem* **2012**, *4*, 307-320; b) H. Makio, H. Terao, A. Iwashita, T. Fujita, *Chem. Rev.* **2011**, *111*, 2363-2449; c) C. Gunanathan, D. Milstein, *Acc. Chem. Res.* **2011**, *44*, 588-602; d) R. H. Crabtree, *New J. Chem.* **2011**, *35*, 18-23.

[4] M. A. Alvarez, B. Alvarez, M. E. García, D. García-Vivó, M. A. Ruiz, *Dalton Trans.* **2013**, *42*, 11039-11042.

[5] S. G. Davies, M. L. H. Green, D. M. P. Mingos, *Tetrahedron* **1978**, *34*, 3047-3077.

[6] a) M. Basato, A. Biffis, G. Buscemi, E. Callegaro, M. Polo, C. Tubaro, A. Venzo, C. Vianini, C. Graiff, A. Tiripicchio, F. Benetollo, *Organometallics* **2007**, *26*, 4265-4270; b) C. W. Liu, Y. S. Wen, L. K. Liu, *Organometallics* **1997**, *16*, 155-157.

[7] R. Liu, X. Zhou, *Chem. Commun.* **2013**, *49*, 3171-3187.

[8] a) L. D. Durfee, I. P. Rothwell, *Chem. Rev.* **1988**, *88*, 1059-1079; b) F. De Angelis, S. Fantacci, A. Sgamellotti*, Coord. Chem. Rev.* **2006**, *250*, 1497-1513.

[9] B. Alvarez, M. A. Alvarez, I. Amor, M. E. García, D. García-Vivó, J. Suárez, M. A. Ruiz, *Inorg. Chem.* **2012**, *51*, 7810-7824.

[10] B. Alvarez, M. A. Alvarez, I. Amor, M. E. García, D. García-Vivó, J. Suárez, M. A. Ruiz, *Eur. J. Inorg. Chem.* **2014**, *51*, 1706-1718.

[11] R. L. Thompson, S. Lee, A. L. Rheingold, N. J. Cooper, *Organometallics* **1991**, *10*, 1657-1659.

[12] F. A. Carey, *Organic Chemistry, 6th Edition,* McGraw-Hill, **2006**, Chapter 17.

[13] Y. Kaya, V. T. Yilmaz, O. Buyukgungor, *Molecules* **2016**, *21*, 52-71, and references therein.

[14] P. Pyykkö, M. Atsumi, *Chem. Eur. J.* **2009**, *15*, 12770-12779.

[15] I. Bernal, S. J. La Placa, J. Korp, H. Brunner, W. A. Herrmann, *Inorg. Chem.* **1978**, *17*, 382-387.

[16] J.-S. Song, D. J. Szalda, R. M. Bullock, *Inorg. Chim. Acta* **1997**, *259*, 161-172.

[17] S. Namorado, M. A. Antunes, L. F. Veiros, J. R. Ascenso, M. T. Duarte, A. M. Martins, *Organometallics* **2008**, *27*, 4589-4599.

[18] B. Cordero, V. Gómez, A. E. Platero-Prats, M. Revés, J. Echevarría, E. Cremades, F. Barragán, S. Alvarez, *Dalton Trans.* **2008**, 2832-2838.

[19] K. Wada, C. B. Pamplin, P. Legzdins, B. O. Patrick, I. Tsyba, R. Bau, *J. Am. Chem. Soc.* **2003**, *125*, 7035-7048.

[20] H. Adams, N. A. Bailey, V. A. Osborn, M. J. Winter, *J. Chem. Soc., Dalton Trans.* **1986**, 2127-2135.

[21] a) J. Honzícek, A. Mukhopadhyay, T. Santos–Silva, M. J. Romao, C. C. Romao, *Organometallics* **2009**, *28*, 2871-2879; b) N. Cabon, F. Y. Pétillon, P. Y. Orain, P. Schollhammer, J. Talarmin, K. W. Muir, *J. Organomet. Chem.* **2005**, *690*, 4583-4601; c) C. G. de Azevedo, M. J. Calhorda, M. A. A. F. de C. T. Carrondo, A. R. Dias, M. T. Duarte, A. M. Galvao, C. A. Gamelas, I. S. Goncalves, F. M. da Piedade, C. C. Romao, *J. Organomet. Chem.* **1997**, *544*, 257-276.

[22] A general trend established for $^2J_{XY}$ in complexes of the type [MCpXYL$_2$] is that $|J_{cis}| > |J_{trans}|$. See, for instance, a) C. J. Jameson, in *Phosphorus-31 NMR Spectroscopy in Stereochemical Analysis*, J. G. Verkade, L. D. Quin, Eds., VCH, Deerfield Beach, FL, 1987, chapter 6; b) B. Wrackmeyer, H. G. Alt, H. E. Maisel, *J. Organomet. Chem.* **1990**, *399*, 125-130.

[23] I. Amor, M. E. García, D. García-Vivó, M. A. Ruiz, D. Sáez, H. Hamidov, J. C. Jeffery, *Organometallics* **2007**, *26*, 466-468.

[24] J. F. Hartwig, *Organotransition Metal Chemistry*, University Science Books, Mill Valley, **2010,** Chapter 9.

[25] For some examples of isocyanide insertion into Mo/W–H bonds to yield formimidoyl derivatives, see: a) M. A. Alvarez, M. E. García, D. García-Vivó, M. A. Ruiz, M. F. Vega, *Organometallics* **2013**, *32*, 4543-4555; b) M. A. Alvarez, M. E. García, A. Ramos, M. A. Ruiz, *Organometallics* **2007**, *26*, 1461-1472; c) N. Cabon, F. Y. Pétillon, P. Schollhammer, J. Talarmin, K. W. Muir, *Dalton Trans.* **2004**, 2708-2719.

[26] D. Pun, E. Lobkovsky, I. Keresztes, P. J. Chirik, *Organometallics* **2010**, *29*, 1789-1796.

[27] When R = *i*Pr, the rotational movement eventually leading to the carbene product **7b** passed first through a new rotamer **C** (4 kJmol^{-1} above **B**) before reaching the corresponding transition state **TS7**. Since the barrier to reach **C** is very low (**TS4** 9 kJmol^{-1} above **B**), the overall rate of the **B**/**7** transformation still is governed by **TS7**, as in all other substrates here studied.

[28] W. L. F. Armarego, C. Chai, *Purification of Laboratory Chemicals*, *7th Edition*, Butterworth-Heinemann, Oxford, U.K., **2012**.

[29] I. Amor, M. E. García, M. A. Ruiz, D. Sáez, H. Hamidov, J. C. Jeffery, *Organometallics* **2006**, *25*, 4857-4869.

[30] a) H. Nishida, N. Takada, M. Yoshimura, T. Sonoda, H. Kobayashi, *Bull. Chem. Soc. Jpn.* **1984**, 57, 2600-2604; b) M. Brookhart, B. Grant, A. F. Volpe Jr., *Organometallics* **1992**, 11, 3920-3922.

[31] *CrysAlis Pro*; Oxford Diffraction Limited, Ltd., Oxford, U. K., 2006.

[32] L. J. Farrugia, *J. Appl. Crystallogr.* **1999**, *32*, 837-838.

[33] (a) G. M. Sheldrick, *Acta Crystallogr., Sect. A* **2008**, *64*, 112-122. (b) G. M. Sheldrick, *Acta Crystallogr., Sect. C* **2015**, *71*, 5-8.

[34] M. J. Frisch, et al., *Gaussian 03, Revision B.02*, see the Supporting Information for the complete reference.

[35] A. D. Becke, *J. Chem. Phys.* **1993**, *98*, 5648-5652.

[36] C. Lee, W. Yang, R. G. Parr, *Phys. Rev. B* **1988**, *37*, 785-789.

[37] P. J. Hay, W. R. Wadt, *J. Chem. Phys.* **1985**, *82*, 299-310.

[38] a) P. C. Hariharan, J. A. Pople, *Theor. Chim. Acta* **1973**, *28*, 213-222; b) G. A. Petersson, A. Bennett, T. G. Tensfeldt, M. A. Al‐Laham, W. A. Shirley, J. Mantzaris, *J. Chem. Phys.* **1988**, *89*, 2193-2218; c) G. A. Petersson, M. A. Al‐Laham, *J. Chem. Phys.* **1991**, *94*, 6081-6090.

[39] a) M. Cossi, V. Barone, R. Cammi, J. Tomasi, *Chem. Phys. Lett.* **1996**, *255*, 327-335; b) A. Fortunelli, J. Tomasi, *Chem. Phys. Lett.* **1994**, *231*, 34-39; c) J. Tomasi, M. Persico, *Chem. Rev.* **1994**, *94*, 2027-2094; d) F. Floris, J. Tomasi, *J. Comput. Chem.* **1989**, *10*, 616-627; e) J. L. Pascual-Ahuir, E. Silla, J. Tomasi, R. J. Bonaccorsi, *J. Comput. Chem.* **1987**, *8*, 778-787; f) S. Miertus, J. Tomasi, *Chem. Phys.* **1982**, *65*, 239-245; g) S. Miertus, E. Scrocco, J. Tomasi, *Chem. Phys.* **1981**, *55*, 117-129.

Entry for the Table of Contents

FULL PAPER

All starts at the Cp ligand! Hydride attack on the cations $[Mo_2Cp_2\{\mu\text{-}\kappa^2_{P,E}:\kappa^1_P,\eta^5\text{-}EP(C_6H_3tBu_3)\}(CNR)(CO)_2]^+$ (E = S, Se) is initiated at the Cp ligand, but eventually reaches the CNR ligand, this being followed by competitive C–C and C–N couplings to the C_6 ring, to yield respectively aldimine and aminocarbene derivatives, the latter being the kinetic product of these reactions (Mo* = $MoCp(CO)_2$; ●= C–*t*Bu)

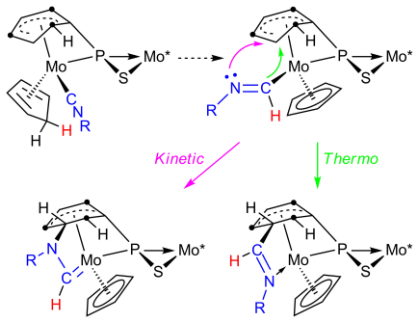

Belén Alvarez, M. Angeles Alvarez, M. Esther García, Daniel García-Vivó, and Miguel A. Ruiz**

Page No. – Page No.

C–C and C–N Couplings Following Hydride Addition on Isocyanide Cyclopolyenyl Dimolybdenum Complexes to Give Tethered Aldimine and Aminocarbene Derivatives